Nonlinear ultrasonic imaging of damage in composite materials using a higher harmonic and modulated multi-path reciprocal method

Salvatore Boccardi, Gian Piero Malfense Fierro, Michele Meo

Department of Mechanical Engineering, University of Bath, Claverton Down BA2 7AY, UK

Abstract

Structural health monitoring (SHM) has become an important factor in the assessment of defects/damage in material components. Ultrasonic methods generally incorporate a sparse array of sensors/transducers, as they provide a low number of piezoelectric sensors per area thus providing savings with regard system costs and weight. Many SHM techniques rely on linear ultrasonic effects such as reflections, amplitude changes, time of arrival and wave scattering effects which rely on precise baseline measurements. In this work, a nonlinear ultrasonic method based on a sparse array of surface bonded ultrasonic transducers was used to evaluate the second harmonic and modulated elastic responses from a damaged medium. A complex composite stiffened panel with barely visible impact damage (BVID) was evaluated. The points closest to damage are found on the paths between transmitter-receiver pairs through a reciprocal relationship of nonlinear elastic parameters and a statistical approach was used to select a cloud of points so that a 2D image of the damaged region is created. Experimental results revealed that the second order nonlinear parameter provided accurate damage localisation and imaging and the use of modulation bands further improved imaging accuracy and damage localisation. The maximum error between the calculated and the real damage area centres was only 1.3 mm. The proposed nonlinear elastic multi-path imaging technique based on higher harmonic generation and modulation coupled with a statistical approach provides damage detection without *a priori* knowledge of the materials characteristics, this is in direct contract to conventional linear ultrasonic methods, which rely on precise measurement of elastic wave effects both before and after the initiation of damage.

Keywords: Composite materials, Structural health monitoring (SHM), Nonlinear damage imaging, Nonlinear Ultrasound, Ultrasound Array, Baseline-Free, Impact Damage, Nonlinear imaging, Modulation, Nonlinear Modulation

1 Introduction

Carbon fibre-reinforced plastic (CFRP) has become a very important material within many industries (aerospace, automotive) due to high strength to weight ratios. CFRP composite materials, however, are susceptible to low velocity impact damage, such as tool drops, as they have the potential to cause hidden damage within the component. This damage is known as barely visible impact damage and contains various types of damage types such as cracks and delamination. Over time, due to the weakening of the mechanical properties the damage can grow and result in failure of the component if no non-destructive inspections (NDI) are carried out. NDI are generally carried out on a periodical basis with the frequency of testing dependent

on the component, this leads to periods where damage may occur and go undetected for long periods of time. Furthermore, NDI testing has a cost associated with it, thus the frequency of testing is limited. All these factors can lead to component failure, which can be costly and/or lead to the loss of life.

There has been a focus on the development of ultrasonic structural health monitoring (SHM) techniques based on *in situ* sparse transducer arrays for early damage detection for aerospace applications. These methods not only reduce maintenance costs but have improved the safety of composite materials [1, 2]. SHM systems are embedded on high value assists (bridges, aircraft) and provide on-demand damage detection and evaluation, furthermore due to advances in electronics there are more reliable components which have facilitated the acceleration in development of compact robust embedded systems [3].

Ultrasonic SHM techniques can be divided into two main fields those relating to linear and nonlinear techniques, linear methods are the conventional methods currently used within industry, while nonlinear methods are recognised for high damage sensitivity and are yet to be fully adopted. Most SHM methods rely on linear effects, such as reflections, phase changes, signal intensity drops, attenuation and group velocity. These methods, while being robust, struggle to determine damage at the micro level scale as they require large barriers to transmission (i.e. large impedance mismatches) and the solving of complex wave scattering and dispersion. Nonlinear ultrasonic methods are based on a direct correlation between the production of higher order harmonics and defects/damage. These nonlinear effects are produced when damage regions are excited with ultrasonic waves, resulting in a clapping/rubbing of the crack interfaces, which lead to nonlinear elastic effects such as higher order harmonics and nonlinear modulations (under dual frequency excitation).

Linear SHM methods rely on many guided wave modes, which result in complicated interference patterns produced by scattering geometric feature and uncertainty in guided wave signals [4]. Linear SHM methods include the reconstruction algorithm for probabilistic inspection of damage (RAPID) [5], the statistical maximum-likelihood estimation [6], delay-sum-imaging and pitch-catch methods [7, 8]. These methods have shown a high level of accuracy for the detection and localisation of damage in both metallic and composite materials. Although, some of the underlining issues with these methods are; importance of specific wave mode excitation/evaluation, accurate determination of time of arrival and baseline measurements on undamaged samples. The consistency and *a priori* knowledge of waveforms on undamaged components and the interactions associated to the damaged component are generally difficult to evaluate, while this is not the case with nonlinear methods due to the direct correlation between the production of higher order harmonics and damage.

Nonlinear modulation occurs when two sinusoidal signals at distinctive frequencies are propagating through a media that has a nonlinear mechanism such as a crack; the mixing of these two propagating waves produces spectral sidebands at the sum and difference between the two frequencies. Lately, the nonlinear behaviour of ultrasonic waves in composite materials has been the main topic of SHM [9-12]. Usually, the second order nonlinear elastic response is used for material damage

localisation [13-15]. Some authors have also considered nonlinear structural responses as sources for damage imaging techniques [16-18] even if this technology can still be considered at an early stage. However, second order nonlinear responses can be generated by laboratory instrumentation which, if not previously calibrated, can disturb the measurements leading to inconsistent results. Recently, several authors, such as Malfense-Fierro and Meo [19], in order to detect damage in multi-layered media, have focused their studies on the modulation effect as it is not affected by instrumentation noise. In this paper, modulation effects are used to improve an existing technique proposed by Boccardi et al. [20], called nonlinear elastic multi-path reciprocal (NEMR) technique. This method was able to localise damage in composite components through a sparse array of surface bonded ultrasonic transducers used to measure the second harmonic nonlinear elastic response associated with the material damage. Although NEMR method was demonstrated to be a reliable and accurate damage localisation technique, it relies on second and higher nonlinear harmonic responses and does not allow damage size estimation.

In this paper, a novel nonlinear ultrasonic SHM technique, called nonlinear elastic multi-path imaging (NEMI) method, is introduced as a natural development of NEMR technique [20]. A sparse array of surface bonded ultrasonic transducers was used to measure the nonlinear elastic responses associated with the material damage. A statistical calculation, applied to the reciprocal relationship of those nonlinear contributions calculated from multiple transmitter-receiver pairs, allowed 2-D damage imaging of a composite component without *a priori* knowledge of structural properties. Hence, the proposed technique allows *both* damage localisation *and* imaging. The paper is outlined as follows: in section 2 the nonlinear parameters involved are introduced and the NEMI method is explained in detail; section 3 shows the experimental set-up; in section 4 it is possible to read the experimental results; in section 5 the main conclusions are discussed.

2 Nonlinear damage imaging for structural health monitoring

2.1 Nonlinear elasticity theory

Composite materials can be affected by contact-type defects, such as micro-cracks and delamination. These kind of defects can be easily understood by introducing a two-dimensional simple model of a contact-type interface (figure 1a) between two rough elastic surfaces [21]. When a stress is applied, the deformation of two opposite sides of the interface (here defined as U_+ and U_-) leads to a change of contact area, generating a nonlinear elastic behaviour. Considering $\varepsilon = U_+ - U_-$ as the variation of thickness of the interface, the internal stress $\Delta\sigma$ can be expressed as a nonlinear spring whose stiffness parameter K is proportional to ε so that $K = K(\varepsilon)$ [21]. The expression of the internal stress $\Delta\sigma$ can be obtained from the spring model by expanding K in a Taylor series approximated to the first order:

$$\Delta\sigma = K\varepsilon = (K_0 + \lambda\varepsilon)\varepsilon = K_0\varepsilon + \lambda\varepsilon^2 \qquad (1)$$

where K_0 and λ are the linear and nonlinear coefficients, respectively. Analysing the interaction of longitudinal ultrasonic waves transmitted along the x-direction (figure 1a) of the composite component, the presence of a defect can be assessed. Thus, a single frequency input wave $u_{SF}(x,z,t)$ is defined as:

$$u_{SF}(x,z,t) = U(x,z)cos(\omega t) \tag{2}$$

where $U(x,z)$ is the amplitude of the deformation, $\omega = 2\pi f$ is the angular frequency, f is the frequency and t is the time. The effective thickness of the crack D is changed by the ultrasonic wave and the variation ε can be expressed as:

$$\varepsilon = D\frac{\partial u_{SF}}{\partial x} = D\frac{\partial U}{\partial x}cos(\omega t) \tag{3}$$

Substituting eq. (3) into eq. (1) leads to:

$$\Delta\sigma = A_0 + A_1 cos(\omega t) + A_2 cos(2\omega t) \tag{4}$$

where

$$A_1 = K_0 D\frac{\partial U}{\partial x} \qquad \text{and} \qquad A_0 = A_2 = \frac{\lambda D^2}{2}\left(\frac{\partial U}{\partial x}\right)^2 = \frac{\lambda}{2K_0}{A_1}^2 \tag{5}$$

Eq. (4) shows how the defect transforms part of the transmitted wave into a nonlinear wave having double of the input frequency (2ω). This is the second order harmonic and its amplitude A_2 can be used as an indication of the presence of a crack. If the transmitted ultrasonic wave has two driving frequencies, in addition to the second harmonic generation, there is another phenomenon, called modulation. A double frequency input wave $u_{DF}(x,z,t)$ can be defined as:

$$u_{DF}(x,z,t) = U_1(x,z)cos(\omega_1 t) + U_2(x,z)cos(\omega_2 t) \tag{6}$$

where $U_1(x,z)$ and $U_2(x,z)$ are the amplitudes of the deformation due to the excitation at angular frequencies ω_1 and ω_2, respectively. At this point, the variation of thickness ε can be now expressed as:

$$\varepsilon = D\frac{\partial u_{DF}}{\partial x} = D\frac{\partial U_1}{\partial x}cos(\omega_1 t) + D\frac{\partial U_2}{\partial x}cos(\omega_2 t) \tag{7}$$

The internal stress for this case can now be defined by substituting eq. (7) into eq. (1) when considering the fundamental, second order and modulated responses:

$$\begin{aligned}\Delta\sigma = {} & A_{0,0} + A_{1,0}cos(\omega_1 t) + A_{0,1}cos(\omega_2 t) + A_{2,0}cos(2\omega_1 t) + A_{0,2}cos(2\omega_2 t) \\ & + A_{1,-1}cos[(\omega_1 - \omega_2)t] + A_{1,1}cos[(\omega_1 + \omega_2)t]\end{aligned} \tag{8}$$

where

$$A_{0,0} = \frac{\lambda D^2}{2}\left[\left(\frac{\partial U_1}{\partial x}\right)^2 + \left(\frac{\partial U_2}{\partial x}\right)^2\right] \quad , \quad A_{1,1} = A_{1,-1} = \lambda D^2\left(\frac{\partial U_1}{\partial x}\right)\left(\frac{\partial U_2}{\partial x}\right) = \frac{\lambda}{{K_0}^2}A_{1,0}A_{0,1}$$

$$A_{1,0} = K_0 D\left(\frac{\partial U_1}{\partial x}\right) \quad , \quad A_{0,1} = K_0 D\left(\frac{\partial U_2}{\partial x}\right) \tag{9}$$

$$A_{2,0} = \frac{\lambda D^2}{2}\left(\frac{\partial U_1}{\partial x}\right)^2 = \frac{\lambda}{2K_0}{A_{1,0}}^2 \qquad \text{and} \qquad A_{0,2} = \frac{\lambda D^2}{2}\left(\frac{\partial U_2}{\partial x}\right)^2 = \frac{\lambda}{2K_0}{A_{0,1}}^2$$

Eq. (8) highlights all the nonlinear parts of the ultrasonic wave due to the presence of the defect. As mentioned before, when a dual frequency ultrasonic wave is transmitted into a damaged medium, each driving frequency leads to a second harmonic component (having amplitude $A_{2,0}$ and $A_{0,2}$) and, in addition, two nonlinear modulated responses are generated at the combination frequencies $\omega_1 \pm \omega_2$. Both the amplitudes $A_{1,1}$ and $A_{1,-1}$ of the modulated terms can be used to assess the presence of a defect. Since $\lambda \ll K_0$, the second order harmonic amplitudes $A_{2,0}$ and $A_{0,2}$ are higher than the modulated responses $A_{1,1}$ and $A_{1,-1}$ (see eqs. (9)) and are usually preferred as nonlinear source for SHM techniques [13, 14]. However, second order harmonics can also be generated by the transmitting instrumentation so that the nonlinear response contains combinations of structural responses and instrumentation noise. Modulated components, even if very small, are not affected by the instrumentation noise and can be considered as a more reliable nonlinear source. In order to allow a higher energy distribution to the modulated bands (figure 1b), the double frequency signal can be created by adding a continuous wave to a sweep. Figure 1b is a representation of an expected response, the production of harmonics can be many orders of magnitude lower than the fundamental response. Figure 1c is shows the time domain signal response along one path between a transducer/sensor pair. The energy of both the second harmonic and modulated windows can be analysed using the acoustic moment α that can be introduced as [22]:

$$\alpha = \int_{\omega_0}^{\omega_0+\Delta\omega} P(\omega)d\omega \qquad (10)$$

where ω_0 is the initial angular frequency, $\Delta\omega$ is the width of the integration window and $P(\omega)$ is the power spectral density.

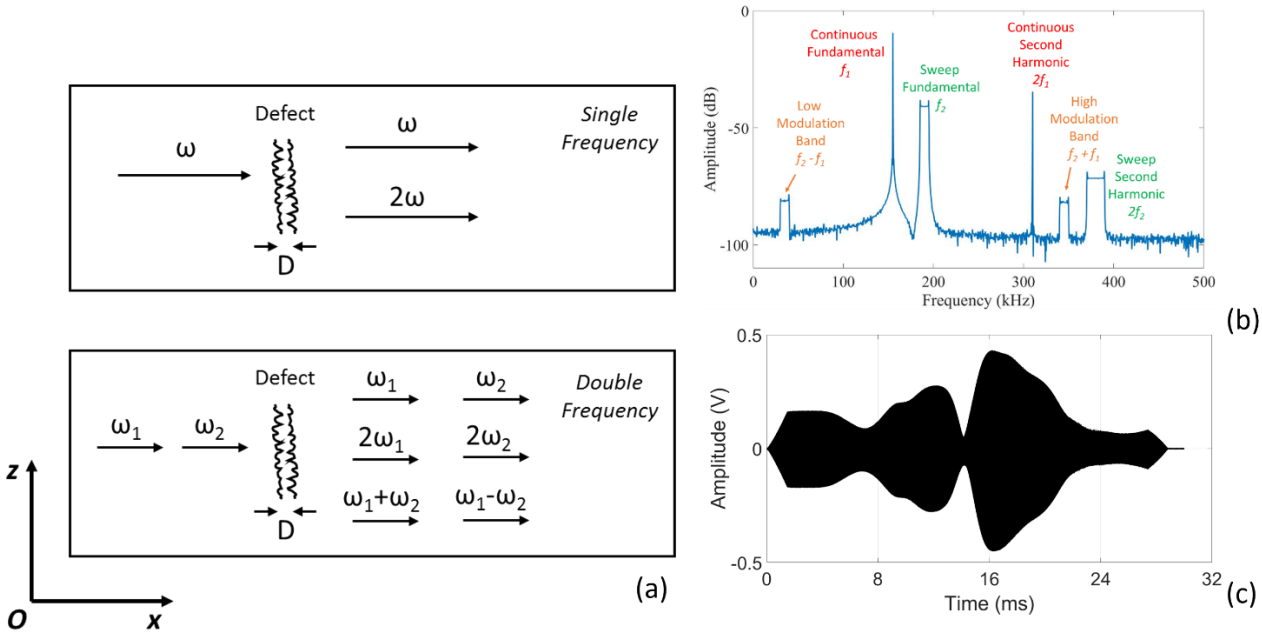

Figure 1. (a) Wave interactions due to the presence of a defect; (b) example of an expected received signal in frequency domain and (c) time domain response of captured frequency sweep.

2.2 Nonlinear elastic multi-path imaging (NEMI)

The nonlinear elastic multi-path imaging (NEMI) method is based on the nonlinear elastic multi-path reciprocal (NEMR) method [20] (briefly described in section 1) and allows the imaging of damage on composite panels. A number N of ultrasonic transducers is placed on a composite plate-like structure with impact damage so that a scanning window is created around the damaged region (figure 2a). As NEMR method, NEMI technique assumes that, due to attenuation, the closer the receiving sensor is to damage, the higher the nonlinear response. Hence, along the path between transmitter-receiver pairs, the point closest to damage (here named point D, see figure 2a) can be localised through a reciprocal relationship [20]. Furthermore, along each path attenuation is equal (S_i to S_j and S_j to S_i), while considering a quasi-isotropic composite panel the attenuation between the sensor pairs may change, the reciprocal relationship will still be valid along the direct paths. The directionality of the travelling wave as well a edge effects are not pronounced and are not expected to greatly effect the results of the direct path, while these effects cannot be totally ignored the statistical method used looks to reduce errors occurring from these effects, furthermore the windowing method used generates larger data sets with the intent of producing more statistically significant results.

Considering the path between sensor i and sensor j (having length L_{ij}), the distance between point D and sensors i and j (L_{iD} and L_{Dj}, respectively) can be calculated as follows [20], which determines the proportionality between the amplitude responses between the two directions:

$$L_{iD} = \frac{L_{ij}\alpha_i}{\alpha_i + \alpha_j} \qquad \text{and} \qquad L_{Dj} = \frac{L_{ij}\alpha_j}{\alpha_i + \alpha_j} \tag{11}$$

where α_i and α_j are the nonlinear responses received by sensor i and sensor j, respectively. Introducing a Cartesian reference frame xOy with origin at the bottom left of the scanning window (see figure 2a), the coordinates of point D (x_{Dij}, y_{Dij}) can be calculated for each transmitter-receiver pair:

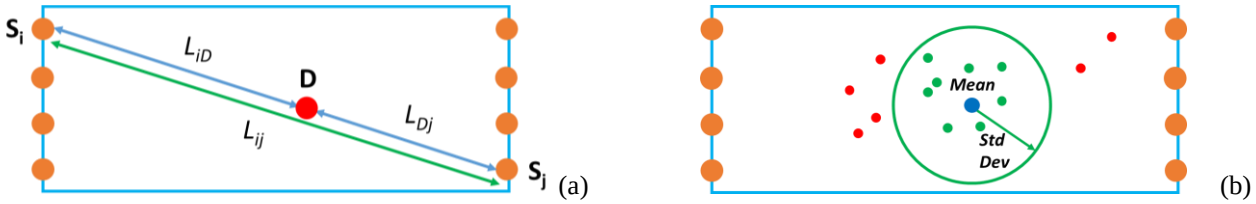

Figure 2. (a) NEMI distance notation in the scanning window and (b) NEMI statistical approach.

$$x_{Dij} = x_i - \frac{L_{iD}}{L_{ij}}(x_i - x_j) = x_i - \frac{\alpha_i}{\alpha_i + \alpha_j}(x_i - x_j) \tag{12a}$$

$$y_{Dij} = y_i - \frac{L_{iD}}{L_{ij}}(y_i - y_j) = y_i - \frac{\alpha_i}{\alpha_i + \alpha_j}(y_i - y_j) \qquad (12b)$$

where (x_i, y_i) and (x_j, y_j) are the coordinates of sensor *i* and *j*, respectively. According to section 2, either second harmonic or modulation response can be used in place of α as input of NEMI method. Eqs. (12) finds the point closest to damage on a single sensor-to-sensor path. Thus, when the nonlinear parameter α is set, the number of *D* points $n_{D\alpha}$ corresponds to the number of paths between sensor pairs and, if *N* sensors are placed on the scanned panel, $n_{D\alpha}$ can be calculated as follows:

$$n_{D\alpha} = \frac{N!}{2!\,(N-2)!} \qquad (13)$$

It should be noted that between a transducer/sensor pair S_i and S_j (figure 2a) material inhomogeneity which affect attenuation and velocity can be neglected (quasi-isotropic layup) due to the same conditions being present between the sensor pair. While these conditions may change between different sensor pairs, the calculation of point D is specific to each path.

If the transmitted signal includes a sweep, the damaged structure will distribute energy to known frequency bands such as the second harmonic and, if the wave has two driving frequencies, high and low modulation (see section 2.1 and figure 1b). Once the frequency band is chosen, it can be split in *k* smaller windows on which the acoustic moment integration can be applied to calculate the nonlinear input parameter α. Hence, there will be $n_{D\alpha}$ points for each window, leading to a total number of *D* points n_D that can be expressed as:

$$n_D = k\frac{N!}{2!\,(N-2)!} \qquad (14)$$

A statistical approach introduced in order to discard points *D* that are wrongly located due to instrumentation faults. At each frequency window, all the point *D* positions are used to create a circular area built by considering their average as a centre $C_\alpha = (x_{C\alpha}, y_{C\alpha})$ and their standard deviation as a radius r_α as follows (figure 2b):

$$x_{C\alpha} = \frac{1}{n_{D\alpha}}\sum_{i=1}^{N}\sum_{j=1}^{i-1} x_{Dij} \qquad y_{C\alpha} = \frac{1}{n_{D\alpha}}\sum_{i=1}^{N}\sum_{j=1}^{i-1} y_{Dij} \qquad r_\alpha = \sqrt{x_{STD\alpha}^2 + y_{STD\alpha}^2}$$

where

$$x_{STD\alpha} = \sqrt{\frac{1}{n_{D\alpha}}\sum_{i=1}^{N}\sum_{j=1}^{i-1}\left(x_{Dij} - x_{C\alpha}\right)^2} \qquad y_{STD\alpha} = \sqrt{\frac{1}{n_{D\alpha}}\sum_{i=1}^{N}\sum_{j=1}^{i-1}\left(y_{Dij} - y_{C\alpha}\right)^2} \qquad (15)$$

All the points *D* outside this circle are discarded. Likewise, another circular area is created from all the averaged C_α points and, if a C_α point is outside the circle, all the points related to its frequency window are discarded. After this process, the output is a cloud of points placed in a smaller region that includes damage. Finally, considering each path of the remaining points *D*, the mean value of the nonlinear contributions α_i and α_j is assigned to the corresponding point *D* so that an image of damage can be created (figure 3).

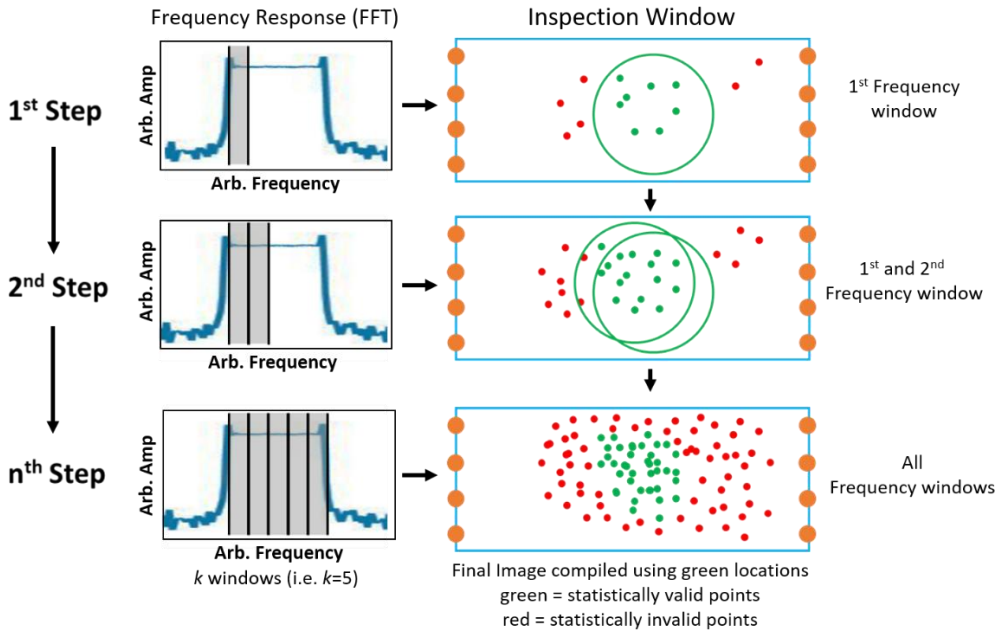

Figure 3.NEMI statistical process.

3 Experimental set-up

The NEMI algorithm for damage imaging, introduced in section 2.2, was experimental validated on an aerospace component. The specimen was an 80 cm x 57.5 cm x 0.5 cm composite curved panel with an unknown lamination sequence, reinforced by three stiffeners and having barely visible damage in three different points (figure 4a). The algorithm was applied on a 14 cm x 30 cm scanning window set between two stiffeners and containing one of the impacted points (C dashed circle in figure 4a). A number of ultrasonic waves were transmitted and received through McWade Acoustic Emission Sensors (dimension of 2 cm x 2.3 cm x 1 cm) having a central frequency of 150 kHz that were placed on two opposite sides of the scanning window (sensor coordinates in table 1). Transducers and sensors were coupled to the sample using ultrasound gel and connected to a National Instruments device used to generate the input signals and capture the received signals (NI PXI-5105 as a waveform generator and NI PXI-5421 as a receiver). A Falco Systems DC 5 MHz High Voltage (WMA-300) amplifier was used to amplify the driving signals whilst a McWade pre-amplifier was introduced to enhance receiving sensor outputs. Three different ultrasonic bursts (time length of 30 ms and amplitude of 300 V peak to peak) were transmitted from each sensor location and received on the opposite side of the scanning region (figure 4b). The first signal was a sine wave sent at a driving frequency of 155 kHz. The second signal was a sweep transmitted by varying the frequency from 185 kHz to 195 kHz. The third signal was built as the average of the first two in order to have modulation. The driving frequencies were chosen so that the nonlinear responses could match as much as possible the central band of the transducers. The structural

responses of these excitations were then measured with a sampling frequency of 5 MHz. The NEMI algorithm was performed using a Matlab code as post-processing manipulation of the recorded signals.

Figure 4c shows the locations of the predicted response for an undamaged section of the panel. When damage is not present the predicted D locations are centred, this is expected as the underlining assumption of reciprocity is met.

Table 1. Sensor coordinates: the origin of the xOy cartesian reference frame is the bottom left corner of the scanning window.

Sensor	x coordinate (cm)	y coordinate (cm)
1	30	11
2	30	8.3
3	30	5.7
4	30	3
5	0	11
6	0	8.3
7	0	5.7
8	0	3

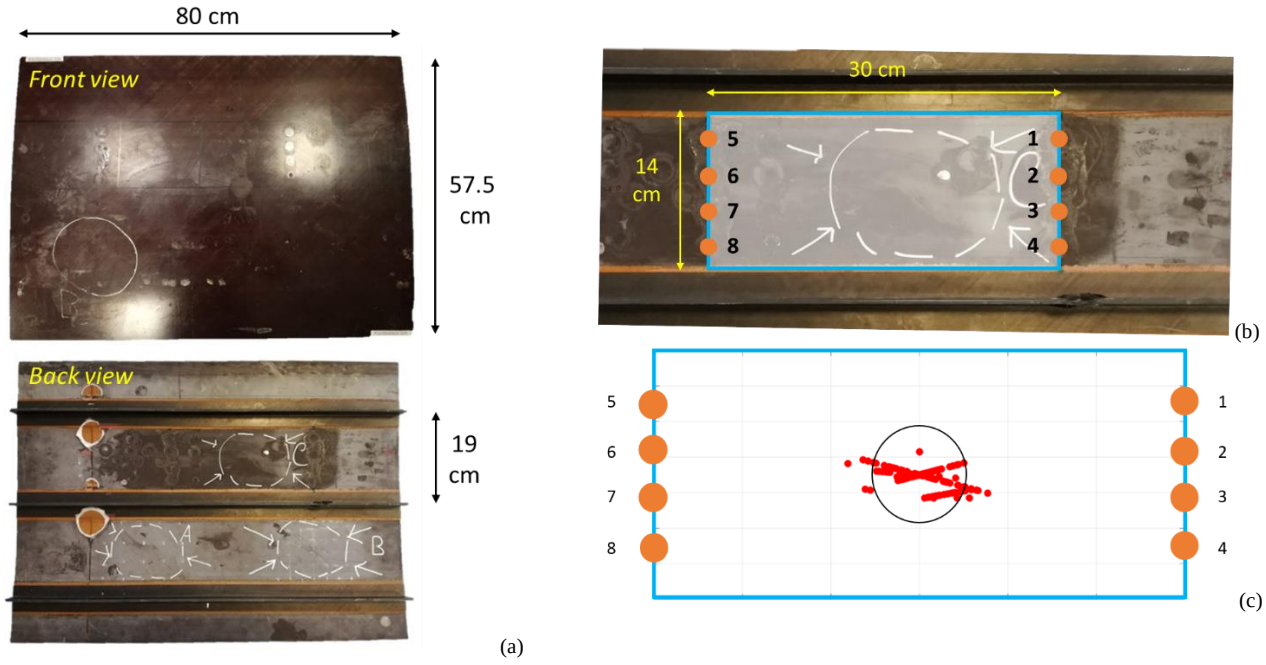

Figure 4. (a) Stiffened composite panel dimensions; (b) scanning window dimensions and sensor positions and (c) evaluation of undamaged area.

4 Experimental Results

4.1 Second harmonic as nonlinear input of NEMI method

NEMI method was performed on a region of a stiffened composite specimen (section 3). The second harmonic window of the 185 kHz – 195 kHz sweep was used to extrapolate the nonlinear inputs of the technique. According to section 2.2, the second harmonic frequency band (between 370 kHz and 390 kHz) was split in k = 10 small windows having a width of 2 kHz ($\Delta\omega$ in eq. 10) so that n_D = 160 points D were located in the scanned region (the paths between sensors on the same side were excluded, see figure 4b). After the statistical cut-out, 19 points D were left, and the image of the damaged region was created by assigning the corresponding nonlinear values. A 50% threshold was used to evaluate the damaged areas (estimated, S_{calc}, and real, S_{dam}) so that the results could be compared to a classical C-scan (figures 5b and 6d, respectively) and the accuracy of the technique could be quantified through two error functions:

$$\xi_{LOC} = \sqrt{(x_{calc} - x_{dam})^2 + (y_{calc} - y_{dam})^2} \tag{16a}$$

$$\xi_{AREA} = \left(1 - \frac{S_{calc} \cap S_{dam}}{S_{dam}}\right) \times 100\% \tag{16b}$$

The function in eq. (16a), ξ_{LOC}, is the distance between the centre of the real damaged area, (x_{dam}, y_{dam}), and the centre of the estimated damaged area, (x_{calc}, y_{calc}), and represents the error in calculating damage location. The function in eq. (16b), ξ_{AREA}, is the percentage of calculated area that does not overlap the real damaged area, used to evaluate the error in calculating damage area imaging and it will be referred as "area imaging error". In the second harmonic case, the maximum localisation error, ξ_{LOC}, was 6.3 mm whilst the maximum area imaging error, ξ_{AREA}, was 21%. This was due to the second harmonic contributions introduced by instrumentation and, in particular, by both McWade and Falco Systems amplifiers.

4.2 Modulated responses as nonlinear input of NEMI method

In order to avoid errors due to instrumentation faults, modulation bands were considered as nonlinear inputs of the method. The double frequency signal was composed of a continuous signal at 155 kHz and a sweep between 185 kHz and 195 kHz, with the second harmonic at 305 kHz, the low modulation band between 30 kHz and 40 kHz and the high modulation band between 340 kHz and 350 kHz. Initially, the single frequency second harmonic was investigated, refer to figure 5. The figure shows that while the second harmonic gives a good indication of the location and size of the damage, it is slightly offset from the actual damage location (figure 5c), which was conducted using a commercially available 128 element ultrasonic phased array scanning system (5MHz Diagnostic Sonar Probe and System).

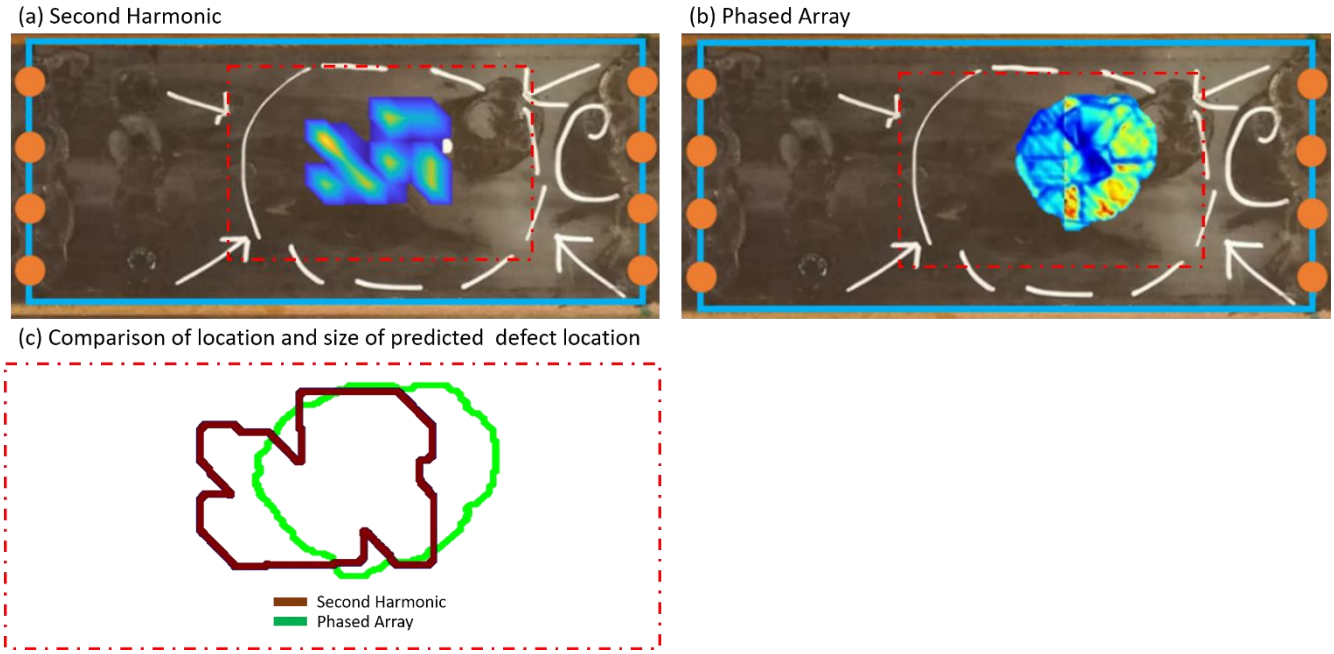

Figure 5. Damage imaging through NEMI method by using the second harmonic (a) compared to a Phased Array C-Scan image (b). A linear interpolation was used as a smoothing algorithm to create a clearer image, with a contour of the relative position and size of the image compared in (c).

For the modulation results, the frequency band was split in k = 10 small windows having a width of 1 kHz and the NEMI technique was performed. Firstly, the nonlinear input was extrapolated from the low modulation band (figure 6a) whilst the second tests involved the high modulation band (figure 6c). Finally, an average of the two modulation contributions was calculated (figure 6b). Figure 6 (a and c) show that the low and average modulation results provide more accurate estimations of the location and size of the damage regions when compared with the phased array results (refer to 6 e and f). From a theoretical point of view, it is expected that the amplitudes of modulated responses are lower than second order nonlinear results but are not affected by equipment-based nonlinearities, thus providing better results for low and average modulation and equivalent for the high modulation when compared with the second harmonic results (figure 5). Furthermore, it should be noted that the high modulation frequency band is more affected by attenuation and thus generally has a lower signal amplitude, in this case resulting in an estimation of the damage region that is not as good as the low modulation results.

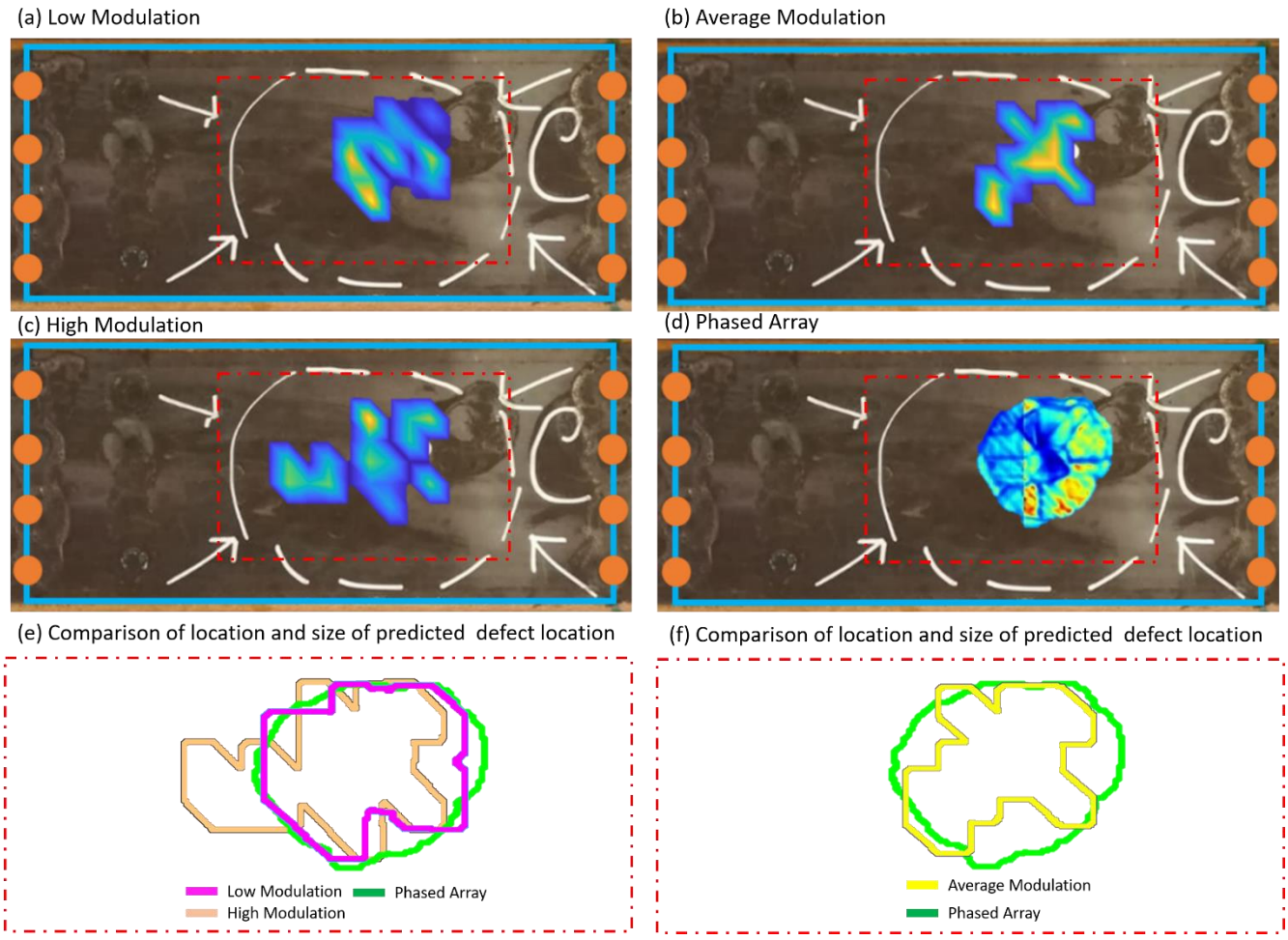

Figure 6. Damage imaging through NEMI method by using different nonlinear contributions low/high modulation (a and c), average modulation (b) and Phased Array C-Scan image (d). A linear interpolation was used as a smoothing algorithm to create a clearer image, with a contour of the relative position and size of the image compared in (e,f).

Table 2 shows localisation and area errors for all cases. The results showed how the introduction of modulated responses led to a general improvement of the imaging of the damage. When high modulation band was used as nonlinear input of NEMI method, although damage localisation error (3.2 mm) resulted decreased in comparison with the second harmonic case (6.3 mm), the error in damage area imaging was higher (29% instead of 21%). This was due to the very low amplitude of the high modulated response since the frequencies involved are far from the central frequency of the transducers. However, when low modulation band was involved, the result was much closer to the real case as damage localisation and imaging errors reduced to 1.8 mm and 6%, respectively. Th low amplitude of the high modulated response also affected the imaging from the averaged nonlinear modulated contributions (ξ_{LOC} = 1.3 mm and ξ_{AREA} = 13%).

Table 2. NEMI localisation and area errors using different nonlinear parameters.

Nonlinear Parameter	Localisation error ξ_{LOC} (mm)	Area error ξ_{AREA} (%)

Second harmonic	6.3	21
Low modulation band	1.8	6
High modulation band	3.2	29
Average of modulation bands	1.3	13

5 Conclusions

This paper introduced a novel nonlinear damage imaging technique for aerospace composite structures, here named nonlinear elastic multi-path imaging (NEMI). This technique can be considered as a development of the nonlinear elastic multi-path reciprocal (NEMR) method and, thus, damage imaging is allowed on composite structures by sending and receiving ultrasonic signals from several surface bonded sensors. Nonlinear parameters, obtained from either second harmonic or modulation bands, are used as input of a reciprocal relationship applied on every path between coupled sensors in order to find the points closest to damage (points *D*, see section 2.2). Once the worst cases are discarded through a statistical approach, the nonlinear parameters are averaged on each path and their values are assigned to the corresponding point *D* so that an image of the damaged component can be built. The second order harmonic is often preferred as nonlinear source for SHM methods since the involved amplitudes are usually the highest. However, modulated responses are also considered for the NEMI technique as, unlike the second order harmonics, they are not affected by instrumentation noise and, thus, they can be considered as a more reliable nonlinear source. The proposed method was experimentally validated on a curved composite structure reinforced by three stiffeners with barely visible damage in three different locations (see section 3). During the first part of the experimental validation, the energy distributed to the second harmonic frequency band was used as the nonlinear input of the technique. Comparing the results to a classical C-scan, the calculated damaged area was slightly shifted leading to a maximum damage localisation error of 6.3 mm. The second part of the experimental campaign involved the use of modulation bands as nonlinear input of the method. Low and high modulation bands, and their average, were used, respectively, to carry out three different sets of experiments. The introduction of modulated responses led to an improvement of damage imaging since the error was reduced to the 1.3 mm by using the low band of the nonlinear modulated contribution. The accuracy of NEMI technique can be considered more than good as it does not require *a priori* knowledge of structural properties such as time of arrival, group velocities of the propagating waveforms nor does it require baseline measurements of the structure. The proposed method leads to better imaging of damaged regions in complex aeronautical structures, resulting in improved reliability and accuracy of aircraft inspection procedures.

References:

[1] Yu, L. and Giurgiutiu, V., In situ 2-D piezoelectric wafer active sensors arrays for guided wave damage detection, *Ultrasonics* **48**, pp. 117-134 (2008).
[2] Kessler, S. S., Spearing, S. M. and Soutis, C., Damage detection in composite materials using Lamb wave methods, *Smart Materials and Structures* **11**, pp. 269 (2002).
[3] Smithard, J., Rajic, N., Van der Velden, S., Norman, P., Rosalie, C., Galea, S., Mei, H., Lin, B. and Giurgiutiu, V., An advanced multi-sensor acousto-ultrasonic structural health monitoring system: development and aerospace demonstration, *Materials* **10**, pp. 832 (2017).
[4] Haynes, C. and Todd, M., Enhanced damage localization for complex structures through statistical modeling and sensor fusion, *Mechanical Systems and Signal Processing* **54**, pp. 195-209 (2015).
[5] Tabatabaeipour, M., Hettler, J., Delrue, S. and Van Den Abeele, K., 11th European conference on non-destructive testing (ECNDT 2014).(2014)
[6] Flynn, E. B., Todd, M. D., Wilcox, P. D., Drinkwater, B. W. and Croxford, A. J., Maximum-likelihood estimation of damage location in guided-wave structural health monitoring, *Proceedings of the Royal Society A: Mathematical, Physical and Engineering Sciences* **467**, pp. 2575-2596 (2011).
[7] Michaels, J. E., Detection, localization and characterization of damage in plates with an in situ array of spatially distributed ultrasonic sensors, *Smart Materials and Structures* **17**, pp. 035035 (2008).
[8] Hua, J., Michaels, J. E., Chen, X. and Lin, J., Simultaneous excitation system for efficient guided wave structural health monitoring, *Mechanical Systems and Signal Processing* **95**, pp. 506-523 (2017).
[9] Ciampa, F., Barbieri, E. and Meo, M., Modelling of multiscale nonlinear interaction of elastic waves with three-dimensional cracks, *The Journal of the Acoustical Society of America* **135**, pp. 3209-3220 (2014).
[10] Hettler, J., Tabatabaeipour, M., Delrue, S. and Van Den Abeele, K., Linear and nonlinear guided wave imaging of impact damage in CFRP using a probabilistic approach, *Materials* **9**, pp. 901 (2016).
[11] Ciampa, F., Pickering, S., Scarselli, G. and Meo, M., Health Monitoring of Structural and Biological Systems 2014, International Society for Optics and Photonics, pp. 906402.(2014)
[12] Jhang, K.-Y., Nonlinear ultrasonic techniques for nondestructive assessment of micro damage in material: a review, *International journal of precision engineering and manufacturing* **10**, pp. 123-135 (2009).
[13] Boccardi, S., CALLA, D., FIERRO, G.-P., Ciampa, F. and Meo, M., Nonlinear Damage Detection and Localisation Using a Time Domain Approach, *Structural Health Monitoring 2015*, (2015).
[14] Ciampa, F., Scarselli, G. and Meo, M., Nonlinear imaging method using second order phase symmetry analysis and inverse filtering, *Journal of Nondestructive Evaluation* **34**, pp. 7 (2015).
[15] Fierro, G. M., Ciampa, F., Ginzburg, D., Onder, E. and Meo, M., Nonlinear ultrasound modelling and validation of fatigue damage, *Journal of Sound and Vibration* **343**, pp. 121-130 (2015).
[16] Ciampa, F., Scarselli, G., Pickering, S. and Meo, M., Nonlinear elastic wave tomography for the imaging of corrosion damage, *Ultrasonics* **62**, pp. 147-155 (2015).
[17] Fierro, G. P. M. and Meo, M., Nonlinear imaging (NIM) of flaws in a complex composite stiffened panel using a constructive nonlinear array (CNA) technique, *Ultrasonics* **74**, pp. 30-47 (2017).
[18] Ciampa, F., Pickering, S. G., Scarselli, G. and Meo, M., Nonlinear imaging of damage in composite structures using sparse ultrasonic sensor arrays, *Structural Control and Health Monitoring* **24**, (2017).
[19] Fierro, G.-P. M., Dionysopoulos, D., Meo, M. and Ciampa, F., Nondestructive Characterization and Monitoring of Advanced Materials, Aerospace, Civil Infrastructure, and Transportation XII, International Society for Optics and Photonics, pp. 105990K.(2018)
[20] Boccardi, S., Calla, D. B., Ciampa, F. and Meo, M., Nonlinear elastic multi-path reciprocal method for damage localisation in composite materials, *Ultrasonics* **82**, pp. 239-245 (2018).
[21] Donskoy, D., Sutin, A. and Ekimov, A., Nonlinear acoustic interaction on contact interfaces and its use for nondestructive testing, *NDT & E International* **34**, pp. 231-238 (2001).
[22] Solodov, I., Bai, J., Bekgulyan, S. and Busse, G., A local defect resonance to enhance acoustic wave-defect interaction in ultrasonic nondestructive evaluation, *Applied Physics Letters* **99**, pp. 211911 (2011).